Archives of Materials Science and Engineering

Volume 28
Issue 12
December 2007
Pages 717-721

International Scientific Journal published monthly as the organ of the Committee of Materials Science of the Polish Academy of Sciences

Superplasticity studies in a beta titanium alloy

M.J. Tan [a,*], X.J. Zhu [a], S. Thiruvarudchelvan [a], K.M. Liew [b]

[a] School of Mechanical and Aerospace Engineering,
Nanyang Technological University, Singapore
[b] Department of Building & Construction,
City University of Hong Kong, China
* Corresponding author: E-mail address: mmjtan@ntu.edu.sg

Received 30.10.2007; published in revised form 01.12.2007

ABSTRACT

Purpose: In the present study, the Superplastic Forming and deformation behavior as well as related mechanisms of this titanium alloy were investigated.

Design/methodology/approach: The high temperature deformation of a beta titanium alloy (Ti-15V-3Cr-3Sn-3Al) was studied in this work. Uniaxial tensile tests were carried out at 650, 750, 850 and 950°C with an initial strain rates from $10^{-1}s^{-1}$ to $10^{-4}s^{-1}$. The effects of temperatures and initial strain rates on the superplasticity of this alloy were studied.

Findings: The studies showed that dynamic recrystallization took place during high temperature deformation and this process not only decrease the average grain size of the alloy but also increase the misorientation angle. Microstructure evolution during high temperature forming as well as related mechanisms were also investigated.

Practical implications: The investigation of microstructure of beta titanium alloy as related phenomens during high temperature deformation are important for achieving desired mechanical behavior of the material.

Originality/value: The Superplasticity studies in a beta titanium alloy as well as related mechanism are investigated.

Keywords: Superplasticity, Dynamic recrystallization; Beta titanium

MATERIALS

1. Introduction

Ti-15V-3Cr-3Sn-3Al (Ti-15-3) alloy is one of the most widely used beta titanium alloys developed in the 1980's [1]. Due to its high strength-to-weight ratio, excellent corrosion resistance and good cold deformability, this alloy has become attractive to many industrial areas such as aerospace and automotive industry [2, 3]. Superplastic Forming (SPF) is a cost-effective process for manufacturing complex shaped structural components [4-14] and SPF of the Ti-15-3 titanium alloy has promising future. Therefore, a better understanding of the superplasticity of this alloy is important for the successful introduction of this material for more industrial applications. Unfortunately, studies on the SPF of Ti-15-3 titanium are limited. In the present study, the SPF and deformation behavior as well as related mechanisms of this titanium alloy were investigated.

2. Experimental details

Ti-15V-3Cr-3Sn-3Al titanium sheets of 1.5mm thickness were used in this study. The chemical composition (wt%) of the present alloy was 3.22 Al, 2.90 Sn, 15.88 V, 0.08 Fe, 3.25 Cr, 0.10 O, 0.008 H, 0.01 C, 0.01 N and the balance was Ti. The as-received alloy has an average grain size of 25 μm determined by linear intercept method using Image Pro+ software. Tensile specimens (dogbone type) with a gauge of 11mm length, 4mm width and 1.5mm thickness were electro-discharged machined with the tensile axis oriented parallel to the final rolling direction. The surfaces of the tensile sample gauge part were polished with silica paste. Uniaxial high temperature tensile tests were performed at 650°C, 750°C, 850°C and 950°C with different initial strain rates. All tests were conducted by first heating up each sample to the desired temperature, and this was followed by a 3 minute holding time to ensure thermal equilibrium. After testing, the deformed specimens were cooled rapidly to room temperature by forced cooling in order to preserve the microstructure. Specimens were sectioned from the gauge as well as grip regions. The samples were polished by silica paste and etched using 10%HF+5%HNO_3+85%H_2O (vol.%) for 5 seconds. For optical study, the linear intercept procedure was employed for measuring the grain size. In the present work, fine grains are defined as grains having a diameter of ≤10 μm. Volume fraction of fine grains ratio measurements were conducted on the gauge section of deformed samples. Images for measurement were first captured by optical microscope. Images were then analyzed using Image Pro+ software. The volume fraction of fine grain ratio was calculated by dividing the fine grain area by the total image area. The electron back scattered diffraction (EBSD) measurements were carried out using a scanning electron microscope (SEM; JEOL 360) equipped with a TSL EBSD system. The SEM was operated at an accelerating voltage of 20kV and EBSD measurements were performed with a step size of 1.0μm.

3. Results and discussion

The variation of elongation-to-failure values as a function of strain rate at different temperatures is shown in Fig. 1. It can be observed from this figure that the optimum condition for deformation of this alloy is at 850°C with an initial strain rate of 0.001/s. A maximum elongation of 305% can be obtained under this condition. It was also observed from this figure that over the temperature range of 650 to 950°C, when the applied strain rate was lower than 0.001/s, the elongation decreases significantly.

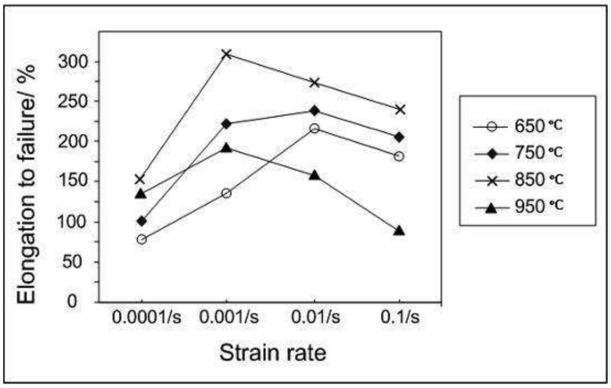

Fig. 1. Variation of elongation-to-failure as a function of strain rate at different temperatures

Fig. 2 shows the graph of log (flow stress) against log (strain rate) at different temperatures. The strain rate sensitivity value, *m*, can be determined from the slope of the curves. The *m* value was approach 0.36 for the sample deformed at 850°C with initial strain rate of 0.01-0.001/s. For the other tests, *m* values were below 0.3. Other studies [15] have shown that for superplasticity to occur, the value of *m* should ideally be within the range of 0.5-0.9, the higher the value, the better the superplastic properties. Within this range, grain boundary sliding is the predominant dislocation mechanism. If *m* value is within the range of 0.3-0.4, elongation would still occur although it would be through the mechanism of recovery controlled dislocation creep, a mechanism which is not very desirable. Lastly, if *m* is less than 0.3, diffusion creep and grain elongation takes place instead of grain boundary sliding. This deformation mechanism leads is not ideal for maximising elongation to deformation. The *m*-value results in Fig. 2 agree with the result of tensile test and it can be deduced from this figure that grain boundary sliding is not the predominant mechanism for this alloy.

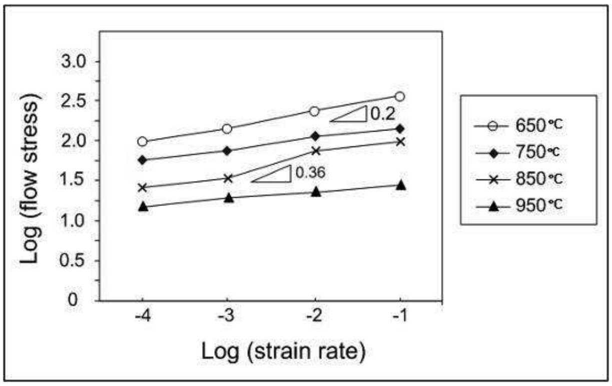

Fig. 2. Graph of Log (Flow stress) against Log (Strain rate) at different temperatures

The microstructures of the deformed sample were examined by optical microscope. Typical microstructure of the grip and gauge parts of sample deformed at 850°C with an initial strain rate of 0.001/s as well as the as-received sample are shown in Fig. 3. It reveals that the grain size of the grip part is much larger than that of the as-received sample. Another phenomenon is that the grain size of the gauge part is much smaller than that of the grip section. Many fine grains were found at the gauge region. These fine grains observed at the gauge region can be presumed as new grains that have been dynamically recrystallized under the influence of stress and elevated temperature. This assumption is valid since the isochronous grains at the grip of the specimen that were not under the influence of stress coarsened.

In order to obtain a better understanding of the dynamic recrystallization phenomenon of this alloy, microstructures of sample deformed at different conditions were examined. The effects of employing different combinations of temperature and strain rate on the percentage of fine grains attainable are shown in Fig. 4 and the average grain sizes of deformed sample are shown in Table 1.

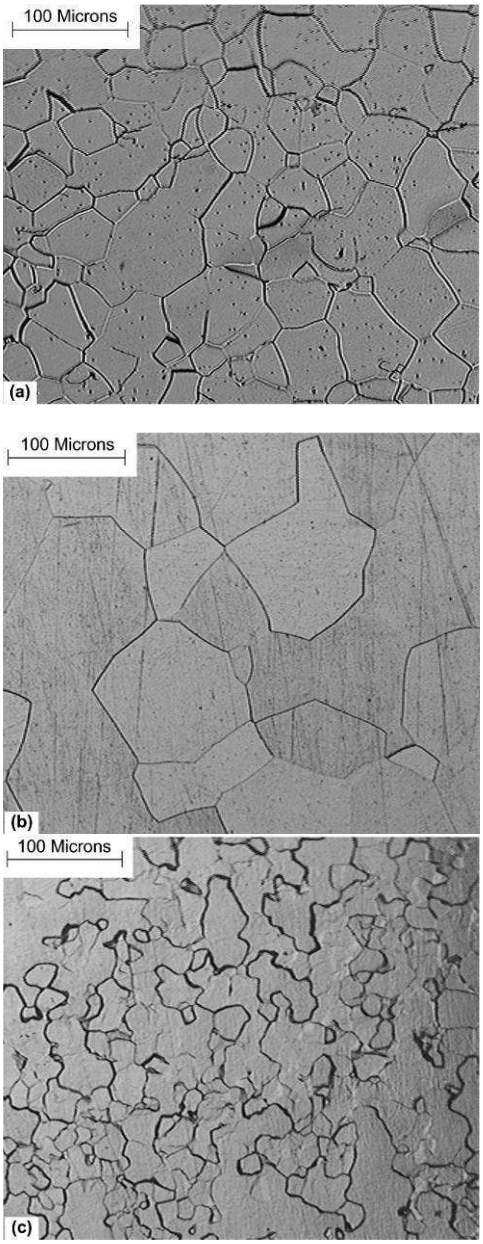

Fig. 3. (a) Microstructure of as-received alloy. Isochronous microstructures at the (b) grip and (c) gauge regions obtained from the same fractured specimen deformed at 850°C and 0.001/s strain rate

It can be seen from Fig. 4 that the highest volume fraction of fine grains can be obtained when the sample is deformed at 850°C with an initial strain rates of 0.001/s. It can also be seen from this figure that grain refinement by dynamic recrystallization becomes less effective at higher test temperature (950°C). This is because the rapid grain growth which offset the positive effects of dynamic recrystallization. Consequently, the percentage of fine grains attainable never exceeds 3% for all the chosen strain rates. It was also difficult to achieve high volume fraction of fine grains at all test temperatures when the strain rate is 0.1/s. This is due to the fact that specimen which deforms at higher strain rates will fail at lower elongation-to-failure; hence the DRX process is incomplete.

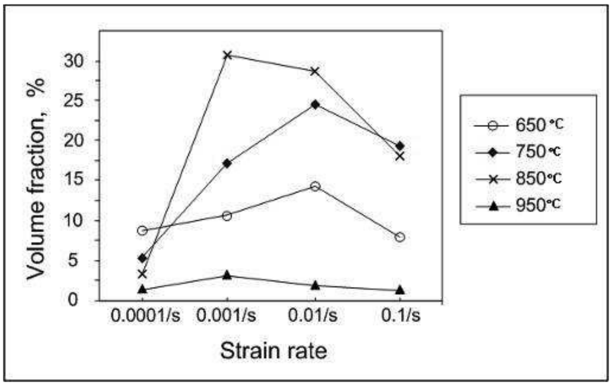

Fig. 4. Volume fraction of fine grains attainable at fracture

Table 1.
Average grain size of different parts of deformed specimen

Test temperature (°C)	Strain rate (s^{-1})	Grain size at grip part (μm)	Grain size at gauge part (μm)
650	1×10^{-1}	31.2	22.6
650	1×10^{-2}	33.6	23.4
650	1×10^{-3}	39.3	22.4
650	1×10^{-4}	49.6	31.6
750	1×10^{-1}	52.3	26.3
750	1×10^{-2}	53.1	24.2
750	1×10^{-3}	56.1	23.3
750	1×10^{-4}	69.8	53.2
850	1×10^{-1}	70.1	52.1
850	1×10^{-2}	71.2	23.3
850	1×10^{-3}	80.2	17.8
850	1×10^{-4}	99.2	58.5
950	1×10^{-1}	89.4	73.2
950	1×10^{-2}	90.6	71.3
950	1×10^{-3}	99.3	77.2
950	1×10^{-4}	112.3	95.6

In order to investigate the dynamic recrystallization phenomenon of the alloy, detailed quantitative evaluation of microstructure was conducted. Samples were strained to different strain levels at 850°C with an initial strain rate of 0.001/s and volume of fine grain fraction was calculated from the gauge parts. Fig. 5 shows the evolution of recrystallized microstructures of the sample deformed at 850°C with an initial strain rate of 0.001/s. At the beginning of the deformation, i.e. ε=0%, because of static grain growth during the heating-up process, the as-received microstructure had transformed into coarse-grained structure with an average size of 70μm. The percentage of fine grains was merely 1% at this stage.

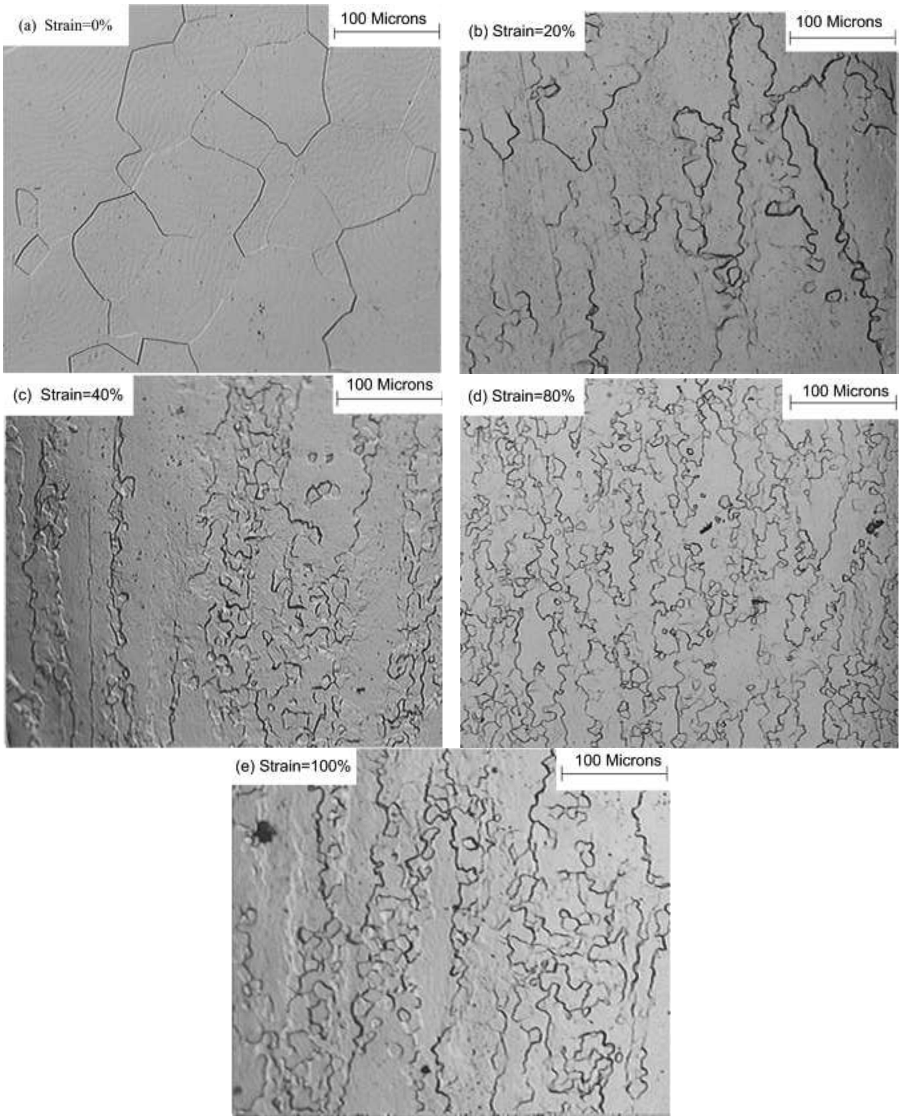

Fig. 5. Micrographs depicts typical microstructural evolution at strain values of (a) 0%; (b) 20%; (c) 40%; (d) 80% and (e) 100% for sample deformed at 850°C with initial strain rate of 0.001/s

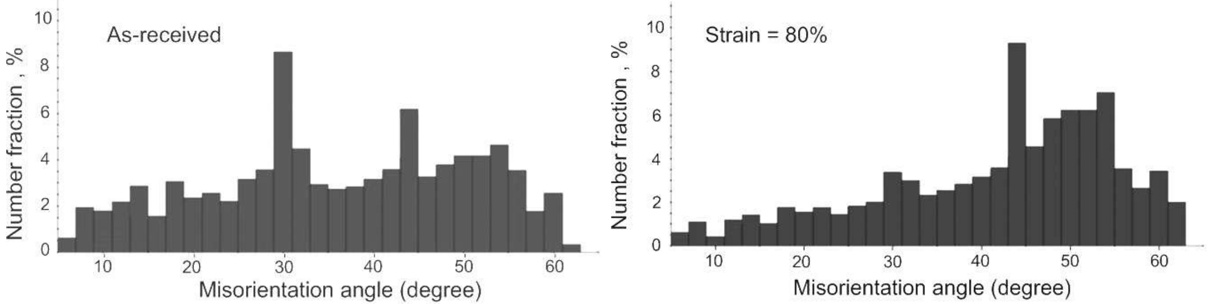

Fig. 6. Histograms showing the misorientation angle distributions of as-received sample and sample strained to 80% at 850 °C with 0.001/s

At ε=20%, some fine grains appear on the grain boundaries. As a result, the average grain size of the sample decreased to 36 μm and the percentage of fine grains increased to 10%. Careful examination of the micrographs show that most of the fine grains are formed along the grain boundaries and the triple points as shown in Fig. 5(b). Fig. 5(c) depicts the microstructure at ε=40%,where the amount of fine grains had increased to 23%. However, the distribution of these fine grains is not homogeneous.

At ε=80% strain level, the amount of fine grains reaches 37%, and the average grain size decreased to 15.1 μm. At this strain level, the average grain size is smaller than that of the as-received sample and the distribution of fine grains is more homogeneous. The results also shown that beyond 80% strain, the percentage of fine grain area decrease while the average grain size increase with increasing strain due to grain growth at this temperature.

EBSD technique was used to investigate the evolution of microstructure characteristics during the tensile test. Fig. 6 shows the distribution of the misorientation angles between 5° and 65° of the as-received sample and sample strained to 80% at 850°C with in initial strain rates of 0.001/s. In this study, we defined the boundaries with a misorientation angle less than 15° as low angle boundaries and those angles greater than 45° are treated as high angle boundaries. The rest within 15°-45° are classified as intermediate angle boundaries. The average misorientation angles deduced from the histograms were 38° and 49° for the as received and deformed sample, respectively. It can also be seen from this figure that the percentages of high angle grain boundaries of deformed samples (40%) is higher than that of the as-received sample (28%).

It is well accepted that grain size is the most important factor affecting superplasticity [15, 16]. Generally, finer the grain size, higher the Superplasticity effect. As discussed earlier, the average grain size is relatively large at the beginning of deformation. This is not favorable for superplastic deformation. However, dynamic recrystallization process not only decreases the average grain size but also increases the average misorientation and these processes are favourable for superplasticity of the material. When deformed at 850°C with an initial strain rate of 0.001/s, maximum volume of fine grains can be obtained. This is the reason why a high elongation-to-failure value can be obtained under this condition.

4. Conclusions

Based on the above mentioned work, the following conclusions can be made:

(1) The optimum deformation condition for this alloy is 850°C with an initial strain rate of 0.001/s. The maximum percentage elongation-to-failure at this condition is 305%.

(2) The strain rate sensitivity ratio, m, of the alloy is lower than 0.36 and grain boundary sliding is not the deformation mechanism of the alloy.

(3) Dynamic recrystallization takes place during 650-950°C and this process not only decreases the average grain size, but also increases the average misorientation angle.

(4) When deformed at the 850°C with an initial strain rate of 0.001/s, the maximum volume of fine grain area is 37% and the average grain misorientation increases from 38° to 49°.

Acknowledgements

The work described in this paper was supported by Nanyang Technological University, Singapore and City University of Hong Kong Strategic Research Grant [Project No. 7001987].

References

[1] D. Hu, A.J. Huang, X. Wu, Sulphide/phosphide precipitation associated with carbon saturation in Ti-15V-3Cr-3Sn-3Al-0.2C, Journal of Alloy Compounds 413 (2006) 77-84.

[2] O.M. Ivasishin , P.E. Markovsky, S.L. Semiatin, C.H. Ward, Aging response of coarse- and fine-grained β titanium alloys, Materials Science and Engineering A 405 (2005) 296-305.

[3] T. Furuhara, T. Maki, T. Makino, Microstructure control by thermomechanical processing in Beta-Ti-15-3 alloy, Journal of Materials Processing Technology 117 (2001) 318-323.

[4] B. Hidalgo-Prada, A.K. Mukherjee, Microstructural Evolution during Superplastic Deformation in a Ni-Modified Ti-6Al-4V Alloy, Scripta Materialia 19 (1985) 1235-1239.

[5] J.S. Kim, J.H. Kim, Y.T. Lee, C.G. Park, C.S. Lee, Microstructural analysis on boundary sliding and its accommodation mode during superplastic deformation of Ti-6Al-4V alloy, Materials Science and Engineering A 263 (1999) 272-280.

[6] A. Arieli, A. Rosen, Plastic flow instability and multiple necking of Ti-6Al-4V during superplastic flow, Scripta Materialia 10 (1976) 809-811.

[7] M.J. Tan, and X.J. Zhu, Dynamic recrystallization in commercially pure titanium, Journal of Achievements in Materials and Manufacturing Engineering, 18 (2006) 183-186.

[8] C.Y. Gao, P. Lours and G. Bernhart, Thermomechanical stress analysis of superplastic forming tools, Journal of Materials Processing Technology 169 (2005) 281-289.

[9] H.L. Xing, K.F. Zhang and Z.R. Wang, A preform design method for sheet superplastic bulging with finite element modeling, Journal of Materials Processing Technology 151 (2004) 284-288.

[10] K.F. Zhang, G.F. Wang, D.Z. Wu and Z.R. Wang, Research on the controlling of the thickness distribution in superplastic forming, Journal of Materials Processing Technology 151 (2004) 54-57.

[11] Z.Y. Ma and R.S. Mishra, Cavitation in superplastic 7075Al alloys prepared via friction stir processing, Acta Materialia 51 (2003) 3551-3569.

[12] A.H. Chokshi and T.G. Langdon, The influence of rolling direction on the mechanical behavior and formation of cavity stringers in the superplastic Zn-22% Al alloy, Acta Materialia 37 (1989) 715-723.

[13] S.N. Patankar, Yeo Thye Kwang and Tan Ming Jen, Alpha casing and superplastic behavior of Ti–6Al–4V, Journal of Materials Processing Technology 112 (2001) 24-28.

[14] Y.M. Hwang and H.S. Lay, Study on superplastic blow-forming in a rectangular closed-die, Journal of Materials Processing Technology 140 (2003) 426-431.

[15] T.G. Nieh, J. Wadsworth, O.D. Sherby, Superplasticity in Metals and Ceramics, Cambridge University Press (1996) 22-50.

[16] O.A. Kaibyshev, Superplasticity of Alloys, Intermetallides and Ceramics, Springer-Verlag (1992) 117-147.